

Quantifying environmental effects on the recruitment of Brazilian sardine (*Sardinella brasiliensis*), 1977-1993*

SILVIO JABLONSKI¹ and LUIZ FERNANDO LOUREIRO LEGEY²

¹ Universidade do Estado do Rio de Janeiro, Departamento de Oceanografia, Rua São Francisco Xavier, 524, Bl. E, 20550-013, Rio de Janeiro, RJ, Brazil; E-mail: jablonski@pobox.com.

² Programa de Planejamento Energético, COPPE, UFRJ, Caixa Postal 68565, 21945-970, Rio de Janeiro, RJ, Brazil E-mail: legey@ppe.ufrj.br.

SUMMARY: The recruitment process for Brazilian sardine (*Sardinella brasiliensis*) from 1977 to 1993 was investigated by taking into account the effects of spawning stock biomass (SSB), the intensity of the wind and the sea surface temperature (SST). Nonparametric models were applied. Best fits resulted from relating recruitment to a combination of SSB and Ekman transport. Transformation of Ekman transport is nearly dome-shaped, with lower and upper limits of 520 and 700 kg s⁻¹ m⁻¹ respectively. Fitting explained 94% of recruitment variability. Regions of maximum values in the transformations were for predictors related to wind, such as wind stress and turbulence index, whose limits were respectively 0.035–0.045 N m⁻² and 30–45 m³ s⁻³. These values correspond approximately to winds of 3.0–4.5 m s⁻¹. SST transformations also follow an apparent dome-shaped curve optimising around 24.75 and 25.5°C. Inclusion of SST as a third predictor variable led to the loss of the dome-shaped relationship, as shown by the transformations with two predictor variables. Biomass curves are almost logarithmic, their critical point oscillating around 200,000–250,000 t, below which value the stock becomes more dependent on recruitment. The biomass range is greater than previous estimates.

Key words: environmental variables, nonparametric models, recruitment, *Sardinella*, Southeastern Brazil.

RESUMEN: CUANTIFICACIÓN DE EFECTOS AMBIENTALES SOBRE EL RECLUTAMIENTO DE LA SARDINA BRASILEÑA (*SARDINELLA BRASILIENSIS*), 1977-1993. – El reclutamiento de la sardina brasileña (*Sardinella brasiliensis*) fue investigado, en el periodo de 1977 a 1993, teniendo en cuenta los efectos de la biomasa del stock frezante, la intensidad del viento y la temperatura de la superficie del mar (TSM). Se aplicaron modelos no paramétricos. Los mejores ajustes fueron obtenidos considerando las variables de biomasa frezante (SSB) y el transporte de Ekman. Para la transformada del transporte de Ekman fue observada una forma aproximada de “domo” con límites inferior y superior, respectivamente, de 520 y 700 kg s⁻¹ m⁻¹. La fracción de la variabilidad del reclutamiento explicada por el ajuste fue de 94%. Fueron evidenciadas regiones de máximo con límites, respectivamente, de 0,035 y 0,045 N m⁻² para el “stress” del viento; y 30 y 45 m³ s⁻³ para el índice de turbulencia. Esos valores corresponden a vientos con intensidad entre 3,0 y 4,5 m s⁻¹. Las transformadas para la TSM muestran, también, un efecto con forma de domo alrededor de 24,75 a 25,5°C. La inclusión de la TSM como una tercera variable independiente llevó a la ‘perdida’ de la forma “domo”, observada en las curvas de las transformadas para dos variables. Para la biomasa, se observan curvas próximas a la logarítmica, con un valor de cerca de 200 a 250 mil toneladas como límite por debajo del cual el stock pasa a depender más estrictamente del suceso del reclutamiento. Ese intervalo es superior a las estimativas obtenidas en estimaciones anteriores.

Palabras clave: modelos no paramétricos, reclutamiento, *Sardinella*, sureste Brasil, variables ambientales.

*Received July 17, 2003. Accepted October 17, 2003.

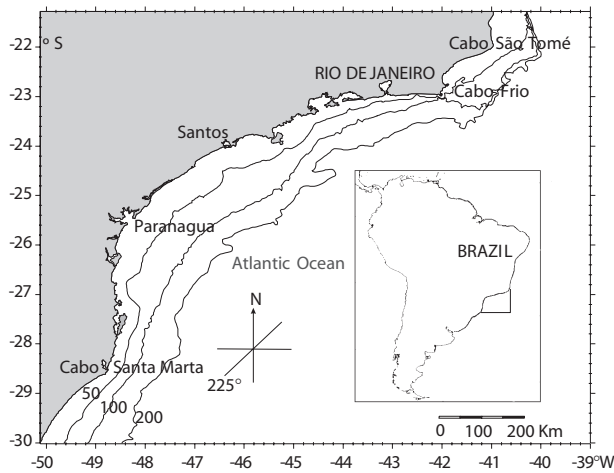


FIG. 1. – The southeastern Brazilian Bight.

INTRODUCTION

The Brazilian sardine (*Sardinella brasiliensis*) supports a commercially important fishery in the southeastern Brazilian Bight (Fig. 1). Catch data are available from 1964. In 1973, the catch peaked at 228 000 t, but since then catches have declined, first to an annual mean of some 140,000 tons from 1977 to 1980 and then to some 125,000 t from 1983 to 1986 (IBAMA, 2000). In 1990, catches were only 32,000 t, but they recovered somewhat to 115,000 t in 1997 before falling again to just 17,000 t in 2000 (Fig. 2). For 2001, partial data indicate a slight recovery, to some 25,000 t.

It is probable that recruitment is influenced by environmental factors related to meteorological and oceanographic conditions of a regional nature, and also to the increase in fishing mortality. According to Matsuura (1996, 1999), limited intrusion of South Atlantic Central Water (SACW) into the Bight in some years negatively influenced the survival of larvae, and hence caused recruitment failure. Brazilian sardine spawn mainly in December and January.

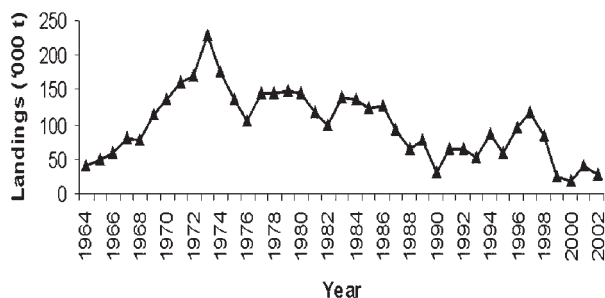


FIG. 2. – Brazilian sardine landings from 1964 to 2000.

Hatching takes place, on average, 19 h after spawning (Matsuura, 1998) and at an age of 45 days juveniles are 40 mm long (Yoneda, 1987). As commercial catches are dominated by sardine aged 1 and 2 years, the effect of poor recruitment is almost immediate.

Cury and Roy (1989), Bakun and Nelson (1991), Roy *et al.* (1992) and Cury *et al.* (1995), applying nonparametric models (Hastie and Tibshirani, 1990), demonstrated the existence of optimal environmental windows, relating wind intensity and recruitment of sardine and anchovy in eastern ocean boundary systems (Morocco, Senegal, Peru, California). The aim of the current work is to follow the example of these authors by presenting an exploratory data analysis using nonlinear techniques. The analyses lead to suggestions of dome-shaped relationships between recruitment success of small coastal pelagic fish in a western upwelling system and low-frequency local wind variability and sea surface temperature (SST).

The intention is later to apply a so-called rule-based model (Bloomer *et al.*, 1994) to the same data set. Such models are constructed so that their output, recruitment (defined as the state variable), is predicted from a set of inputs known as driving variables (in this case, spawning stock biomass and environmental variables), using different weights derived from the correlation between state and driving variables. The idea here is to validate some of the results obtained with nonparametric statistical techniques that are not entirely consistent owing to uncertainties related to the small size of the data set.

MATERIAL AND METHODS

The position of the SACW front was determined by the position of the 18°C isotherm near the seabed. Data for this purpose were obtained from the “Integrated project for the use and rational exploitation of marine environment” (IOUSP/ FINEP), covering the period 1975–1982 and the area between Cabo Frio (23°S) and Cabo Santa Marta (29°S). Cruises carried out between 1976 and 1980 yielded data suitable for establishing temperature profiles. Wind stress, wind intensity and SST were taken from the Atlas of Surface Marine Data 1994 (Da Silva *et al.*, 1994), which provides monthly averages with a spatial resolution of 1° longitude and 1° latitude.

Ekman transport ($\text{kg s}^{-1} \text{m}^{-1}$) was calculated from Stress / f , where f is the Coriolis parameter and Stress the wind stress. Ekman transport was derived

from the wind stress component parallel to the coastline, i.e. approximately 225°, so making it more representative of reality (Sunyé, 1999). The turbulence index (wind speed cubed) was calculated to represent the rate at which wind energy is added to the ocean to produce turbulent mixing of the upper water column (Cury and Roy, 1989; Bakun and Parrish, 1990).

Values of spawning stock biomass and recruitment were taken from the data provided by Cergole (1993) and Cergole *et al.* (2002), who used Virtual Population Analysis (VPA; Gulland, 1965) to determine them. Natural mortality ($M = 1.2 \text{ year}^{-1}$) was derived from Pauly's (1980) empirical equation, using documented growth parameters of sardine and average water temperature in the Brazilian Bight (Cergole, 1995; Cergole *et al.*, 2002). Spawning stock biomass is taken to be the sum of the mature portion of each age class. According to Cergole (1993), 50% of age class 1, 75% of age class 1.5 and 100% of age class 2 and older sardine are mature. Recruitment was taken to be the number of sardine attaining 0.5 years of age.

Estimates of recruitment and spawning stock biomass were available from 1977 to 1997, but owing to uncertainties in the VPA methodology, only recruitment values up to 1995 are considered reliable (Cergole *et al.*, 2002). Further, estimates of the average zonal and meridional wind stress were only available up to 1993 (Da Silva *et al.*, 1994). These data are of a better quality than those available at the COADS (Comprehensive Ocean–Atmosphere Data Set). The wind parameters in the Da Silva database are based on a new scientific Beaufort equivalent scale, so they yield improved resolution and boundary layer parameterisation. To be able to use two more points (1994 and 1995) in the analysis would require the use of values of wind stress from COADS, but the available figures at COADS correspond to pseudo-stress, which does not consider the constants for air density and the empirical drag coefficient. Therefore, we decided to use just 17 points rather than 19, taking into account only the values for wind stress we consider to be more reliable.

Knowledge of the causal factors defining the relationship between a dependent variable and its possible predictors is not always sufficient to establish its form *a priori*. In such cases, nonparametric statistical methods can be used to establish a functional form between response and predictor variables, taking into account the data themselves (Cury *et al.*, 1995). Generalised additive models (GAM;

Hastie and Tibshirani, 1990) use iterative algorithms to generalise multiple linear regression analysis.

Additive models

Additive models generalise the linear model in such a manner that part or all of its predictor's linear functions are substituted by arbitrary smoothers. The linear model

$$Y = \sum_{i=0}^n \beta_i X_i + \varepsilon,$$

is substituted by the additive model

$$Y = \alpha + \sum_{i=1}^n f_i(X_i) + \varepsilon$$

where, as in the linear model, errors ε are independent of X_i . $E(\varepsilon) = 0$, $\text{var}(\varepsilon) = \sigma^2$ and f_i are univariate arbitrary functions (e.g. smoothing functions), one for each predictor. When not specified, the smoothing spline was used instead of other smoothers because it seemed to indicate trends more appropriately.

The additive models retain an important feature of the linear models, namely the separability of responses. This means that the variation of the fitted response surface, holding all but one predictor fixed, does not depend on the values of the other predictors. Therefore, it is possible to plot the n functions separately after fitting, and to examine the role of each predictor in modelling the response (Hastie and Tibshirani, 1990).

As in the linear model, we keep the model as simple as possible. In a parametric model, one degree of freedom (d.f.) is used to estimate each coefficient generated for each of its terms. Models that include smoothed terms use both parametric and nonparametric degrees of freedom. The difference between the number of observations and the degrees of freedom required to fit the model is referred to as the residual degrees of freedom.

Response transformation models

Another approach involving response transformation models was used in this paper to obtain nonparametric regressions. Their general form is

$$\theta(Y) = \alpha + \sum_{j=1}^n f_j(X_j) + \varepsilon,$$

where ε has a mean of zero and is independent of X_j . The transformation $\theta(Y)$ and the functions $f_j(X_j)$ are arbitrary smoothers.

Two methods were used to fit the data, ACE (Alternating Conditional Expectations; Breiman and Friedman, 1985) and AVAS (Additivity and Variance Stabilisation; Tibshirani, 1988). ACE is a non-parametric generalisation of the additive model that fits a model as part of an alternating estimation procedure. If Y and X are random variables and we need to obtain the transformations $\theta(Y)$ and $f(X)$ so that $E\{\theta(Y)|X\} \approx f(X)$, ACE tries to find the best fit solution by minimising the squared error $E\{\theta(Y) - f(X)\}^2$. Some of the ACE properties can lead to anomalies (Breiman and Friedman, 1985; Hastie and Tibshirani, 1990; Cury *et al.*, 1995). For a single prediction, ACE is symmetrical in X and Y , which is not expected in regression procedures. Hastie and Tibshirani (1990) suggest that ACE would be a more adequate tool for correlation than regression issues. In addition, ACE exhibits strange behaviour in low-correlation settings, which may affect results even in a regression context.

AVAS is a modification of ACE that is designed specifically for regression problems. The basic difference is that AVAS uses an asymptotic variance-stabilising technique. Given the random variables Y and X_1, \dots, X_p , the aim is to obtain transformations $f_1(X_1), \dots, f_p(X_p)$ and $\theta(Y)$, so that

$$E\{\theta(Y)|X_1, \dots, X_p\} = \sum_{j=1}^p f_j(X_j)$$

and

$$\text{var}\left\{\theta(Y)\left|\sum_{j=1}^p f_j(X_j)\right.\right\} = \text{constant}.$$

The AVAS procedure alternates two steps, one to determine the mean function given the response transformation, and the second to determine the variance transformation given the mean.

For both ACE and AVAS, the linearity of the relationship between the transformation θ and $f_j(X)$ indicates whether an adequate fit was achieved. It is necessary to bear in mind that, when fitting a linear model, it is possible to obtain an analytical

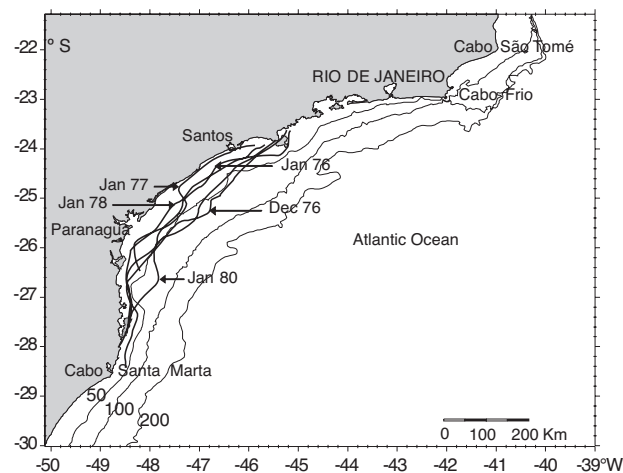


FIG. 3. – The SACW front delineated by the 18 °C bottom isotherm, from cruises FINEP II (01/76), FINEP V (12/76), FINEP VI (01/77), FINEP VII (01/78) and FINEP XI (01/80). The front is indicated by the lines associated with each cruise date.

expression, but that the same does not apply to additive models using smoothers. The form of the transformations is obtained by plotting the new transformed values of Y and X_j against the original observed values.

Recruitment was used as the response variable for the application of additive models (GAM, ACE and AVAS). For predictor variables we used spawning stock biomass (SSB), average Ekman transport, wind stress, turbulence index and SST for January and for December of the previous year, covering the peak period of spawning of sardine in the southeastern Brazilian Bight. Results were obtained for each predictor separately and for combined variables.

RESULTS

Figure 3 shows the position of the SACW front delineated by the 18°C bottom isotherm for five cruises from 1976 to 1980. Its distance from the coast varied with latitude, but its proximity to the coast was greatest in January 1977 and 1978. The

TABLE 1. – Mean distance from the coast of the 18°C bottom isotherm for each cruise, and average values of wind stress, wind speed, Ekman transport and turbulence index. Source: Project IOUSP/FINEP; Atlas of Surface Marine Data 1994; Da Silva *et al.* (1994).

Cruise	Date	Distance (km)	Wind stress (N m ⁻²)	Ekman transport (kg s ⁻¹ m ⁻¹)	Wind speed (m s ⁻¹)	Turbulence index (m ³ s ⁻³)
FINEP II	January '76	31.62	0.032	512.73	3.50	42.87
FINEP V	December '76	47.92	0.020	155.41	2.47	15.08
FINEP VI	January '77	28.66	0.045	405.14	4.78	108.90
FINEP VII	January '78	22.66	0.025	348.58	3.02	27.61
FINEP XI	January '80	54.79	0.019	102.14	1.83	6.10

TABLE 2. – R^2 and p -values for the linear regressions between the distance of the SACW front from the coast and different predictor variables. The best fit is emboldened.

Parameter	R^2	p -value
Wind speed	0.39	0.258
Wind stress	0.54	0.159
Ekman transport	0.70	0.079
Turbulence index	0.34	0.306

distance between the SACW front and the coast was depicted graphically at intervals of 0.25° latitude, and the simple mean was calculated. Only the interval limited by 24 and 28°S , for which there were available data for all cruises, was accounted for.

Table 1 relates the mean distance of the SACW front for each cruise to the average values of wind stress, wind speed, Ekman transport and turbulence index. The apparent discrepancy observed for the values of Ekman transport and mean wind speed in January 1976 compared with the same variables in other periods can be explained by the stronger wind at low latitudes that year, which thus generated a higher value for transport.

Table 2 illustrates the results (R^2 and p -values) of the linear regressions between the average distance between the SACW front and the coast and wind speed, wind stress, Ekman transport and turbulence index. Despite the few observations (just 5 points), the R^2 for the relationship with wind stress and Ekman transport are both high. However, the corresponding p -values are 0.08 and 0.16 , which would not support a rejection of the null hypothesis at an error level of 5% .

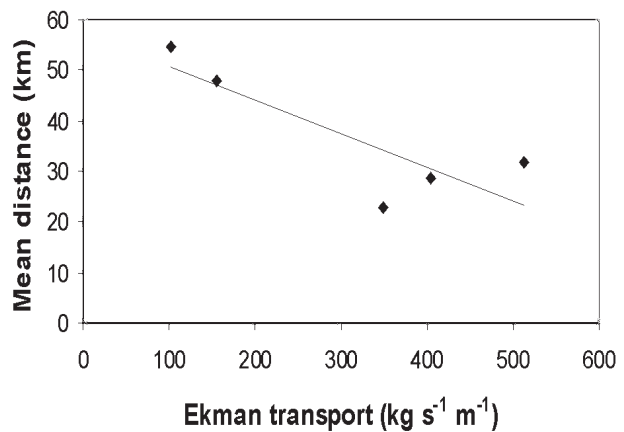


FIG. 4. – Relationship between Ekman transport and the mean distance of the SACW front from the coast.

TABLE 3. – Recruitment and spawning stock biomass of Brazilian sardine, 1977–1993. Source: Cergole (1993) and Cergole *et al.* (2002).

Year	Recruitment (billions)	Spawning stock biomass (10^3 ton)
1977	18.6	394
1978	16.5	394
1979	16.8	302
1980	12.6	249
1981	23.0	195
1982	23.8	278
1983	22.1	371
1984	20.7	407
1985	14.3	317
1986	12.2	255
1987	10.9	177
1988	7.2	165
1989	3.8	118
1990	16.9	219
1991	30.2	290
1992	22.8	419
1993	16.6	344

TABLE 4. – Average wind speed, wind stress and turbulence index, Ekman transport and SST in the area of the continental shelf off south-eastern Brazil (22 – 29°S), out to roughly the 200 -m isobath. These data were used to fit the GAM, ACE and AVAS models. Source: Atlas of Surface Marine Data 1994; Da Silva *et al.* (1994).

Year	Wind speed (m s^{-1})	Stress components		Stress (N m^{-2})	Ekman transport ($\text{kg s}^{-1} \text{m}^{-1}$)	Turbulence index ($\text{m}^3 \text{s}^{-3}$)	SST ($^\circ\text{C}$)
		Zonal	Meridional				
1977	3.70	-0.0331	-0.0034	0.0333	439.0	50.81	25.21
1978	3.16	-0.0257	-0.0149	0.0296	479.9	31.61	25.08
1979	2.68	-0.0232	0.0063	0.0241	204.8	19.33	24.32
1980	2.86	-0.0302	-0.0110	0.0322	495.9	23.41	24.63
1981	3.28	-0.0316	-0.0144	0.0347	549.3	35.24	25.15
1982	2.64	-0.0255	-0.0016	0.0256	329.0	18.40	24.74
1983	2.62	-0.0249	-0.0162	0.0297	487.2	18.02	25.48
1984	3.18	-0.0262	-0.0172	0.0313	512.4	32.22	25.39
1985	3.62	-0.0255	0.0057	0.0262	240.6	47.30	23.80
1986	3.40	-0.0308	-0.0105	0.0326	501.0	39.20	24.49
1987	3.52	-0.0221	-0.0174	0.0281	537.8	43.62	24.97
1988	3.25	-0.0272	-0.0089	0.0287	438.8	34.26	25.48
1989	3.84	-0.0368	-0.0260	0.0451	749.2	56.78	24.44
1990	4.22	-0.0388	-0.0148	0.0415	635.8	74.96	24.39
1991	3.41	-0.0383	-0.0096	0.0395	566.7	39.82	24.98
1992	2.81	-0.0204	0.0029	0.0206	221.0	22.09	25.12
1993	3.41	-0.0267	-0.0076	0.0277	407.0	39.66	24.85

Figure 4 portrays a scatter plot for the five cruises, relating Ekman transport to the mean distance between the SACW front and the coast. Again despite the fact that observations were few, it was possible to demonstrate the existence of a linear relationship between the offshore-directed wind-driven surface transport and the position of the SACW front in the study region. The results indicate that winds in the range $3.0\text{--}4.5\text{ m s}^{-1}$ (Ekman transport $350\text{--}500\text{ kg s}^{-1}\text{ m}^{-1}$) seem to be strong enough to bring the SACW front in towards the coast. Considering the effective role of Ekman transport in the

SACW intrusion and the consequent enrichment and stability of the water column, it is therefore possible to analyse the influence of environmental conditions, in this case wind intensity, on the recruitment process.

Values of spawning stock biomass (SSB) and recruitment (R) are given in Table 3. Table 4 lists the annual average wind speed, wind stress, Ekman transport, turbulence index and SST for the southeastern Brazilian continental shelf ($22\text{--}29^\circ\text{S}$, out to roughly 200 m deep). These were the data used in the nonparametric models.

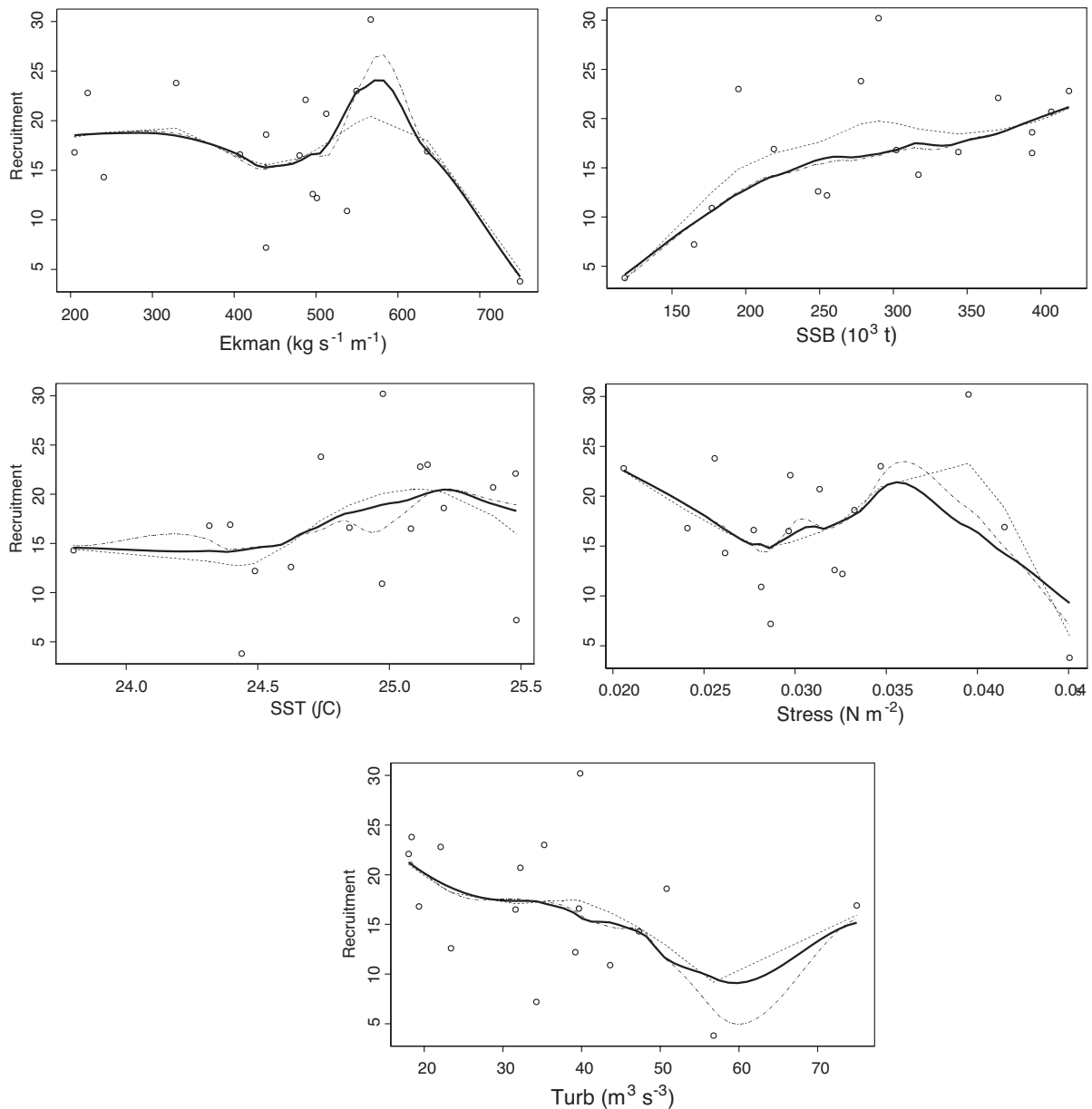


FIG. 5. – Recruitment as a function of possible predictor variables – spawning stock biomass (SSB), Ekman transport (Ekman), turbulence index (Turb), wind stress (Stress) and sea surface temperature (SST). A trend line was fitted with smoothers (lowess with span = 0.50 – dot-and-dashed line; lowess with span = 0.55 – solid line; smooth spline – dashed line). The points are observed values. Recruitment is given in billions of sardine.

Figure 5 shows recruitment variation as a function of possible predictor variables, namely spawning stock biomass (SSB), Ekman transport (Ekman), turbulence index (Turb), wind stress (Stress) and sea surface temperature (SST). A trend line was fitted by means of smoothers: lowess, locally weighted scatterplot smoother with span 0.50 and 0.55, and smooth spline (Hastie and Tibshirani, 1990). The fitted curves give an initial insight of the functional form of the relationship between the variables.

The relationship between recruitment and spawning stock biomass has a similar shape to that suggested by the Beverton and Holt (1957) model. Fitting for Ekman transport and wind stress reveals a dome-shaped region limited, respectively, by 500 and 600 kg s⁻¹ m⁻¹ and 0.035 and 0.042 N m⁻², which corresponds to an average wind speed of 3.0–4.5 m s⁻¹. For the turbulence index, the curves do not show any clear pattern. The SST curve has also a dome-shaped region between 24.5 and 25.5°C.

Additive models

Generalised additive models and those with response transformation were fitted to data by means of S-PLUS (1997) routines (GAM, ACE and AVAS). The form of the fit was achieved by plotting the new transformed values against the original values. The models were applied to each predictor variable separately (figures not presented) and then incorporating SSB to each of the environmental variables (Ekman transport, turbulence index, wind stress and SST). We also modelled the effect of SST combined with SSB and each of the variables related to the wind.

Table 5 presents the values of R^2 , for ACE and AVAS fits, corresponding to the fraction of the vari-

ance in recruitment explained by the fit, and the residual deviance for GAM. In this case fit quality is measured by the residual deviance, the best fit matching the lowest residual. R^2 values for the multiple linear regressions are also presented for comparison. Cury *et al.* (1995) stress that the results for any of these algorithms should be viewed with caution because of the assumptions underlying each model. One way to deal with that situation is to compare the different results for the same data set, taking into account also the need to be consistent in the knowledge of the phenomena it is intended to model.

Figures 6, 7 and 8 illustrate the transformations, showing the combined effects of SSB and each of the environmental variables. The transformations for recruitment and spawning stock biomass are practically identical in all fits. They are therefore illustrated only for the first case (SSB and Ekman). The same similarity is evident with the fits for ACE and AVAS, so only the curves resulting from ACE are presented. For SSB and Ekman transport, the transformations of the three models are very close (Fig. 6), indicating for Ekman transport a region of peak values limited by 500 and 700 kg s⁻¹ m⁻¹. For SSB and the turbulence index, the resulting transformations from ACE and AVAS show opposite trends for values >40 m³ s⁻³ (Fig. 7). When the point corresponding to the year 1990 (75 m³ s⁻³, with a high s.e. – see GAM transformation in Fig. 8D) is disregarded in applying ACE, the shapes of the two transformations (AVAS in Fig. 7B and ACE in Fig. 8C) are similar, with a discrete peak between 35 and 45 m³ s⁻³. This suggests that ACE could be more susceptible than AVAS or GAM to values in the upper portion of the distributions (or with larger s.e.). AVAS seemed not to respond to the elimination of

TABLE 5. – Coefficients of determination R^2 for the application of the ACE and AVAS methodology, the residual deviances for the GAM, and coefficients of determination R^2 for the linear multiple regression.

Parameters	ACE (R^2)	AVAS (R^2)	Residual deviance	GAM		Linear regression		
				Residual d.f.	p-value*	(R^2)	F	p-value**
SSB	0.88	0.62	323.26	11.999	0.198	0.32	7.0350	0.01811
Ekman	0.69	0.21	399.77	11.999	0.112	0.06	1.0100	0.33090
TSM	0.23	0.20	501.98	11.999	0.412	0.08	1.3800	0.25840
Stress	0.58	0.12	309.91	12.000	0.022	0.03	0.3982	0.53750
Turb	0.37	0.12	499.05	12.001	0.461	0.11	1.8700	0.19160
SSB+TSM	0.89	0.77	178.94	7.998		0.34	3.6170	0.05416
SSB+Stress	0.88	0.61	180.04	7.999		0.34	3.5720	0.05580
SSB+Ekman	0.94	0.83	183.67	7.998		0.32	3.3240	0.06587
SSB+Turb	0.88	0.67	284.87	8.001		0.34	3.5330	0.05727

ACE: Alternating Conditional Expectations; AVAS: Additivity and Variance Stabilisation; GAM: Generalised Additive Model.

* Only p-values for the fits with one predictor variable are shown. For the multiple fits, the GAM shows one p-value for each predictor variable.

** p-value for F test.

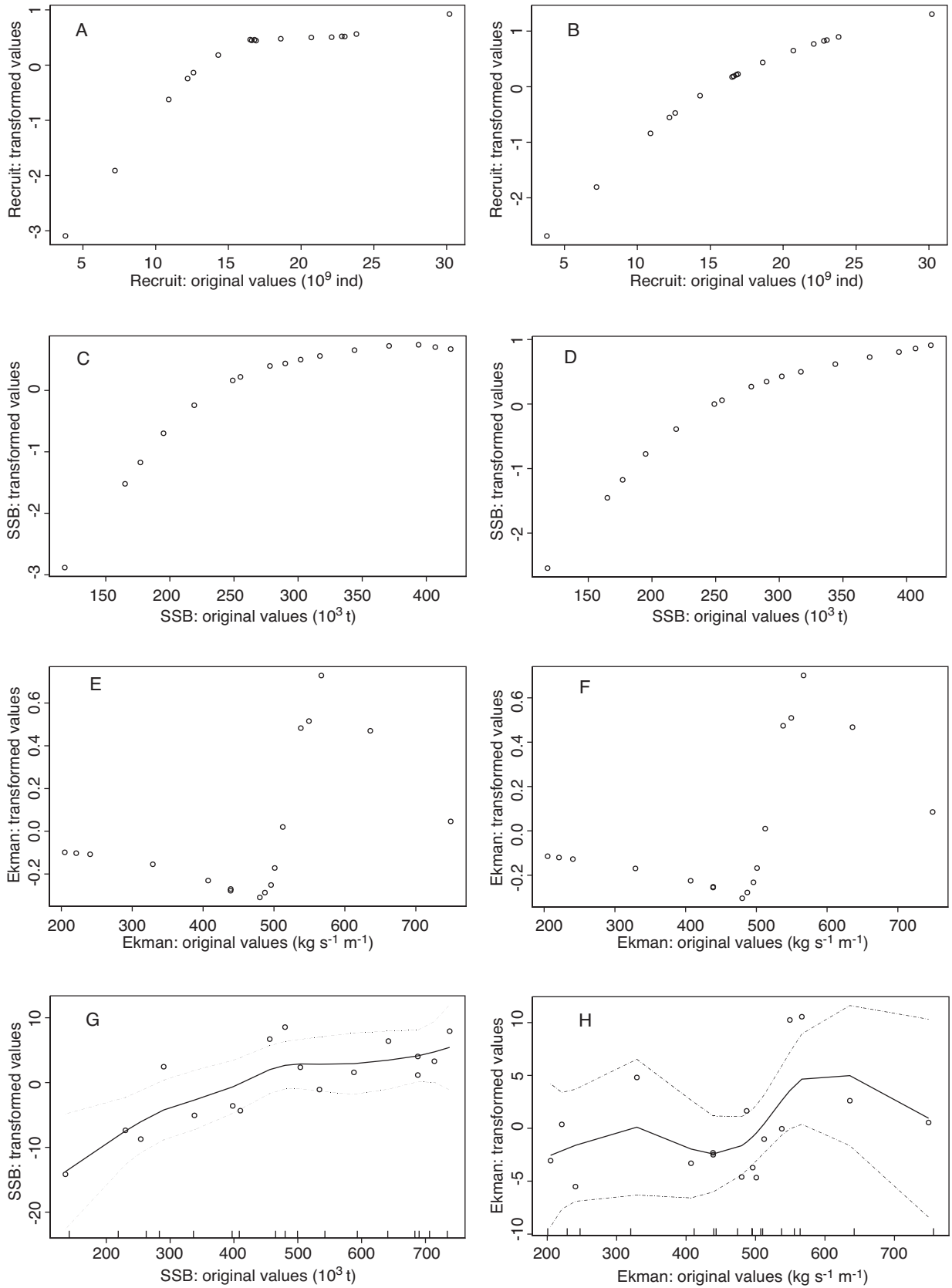


FIG. 6. – ACE transformations for (A) recruitment, (C) SSB and (E) Ekman transport, AVAS transformations for the same variables (6B, 6D, 6F), and GAM transformations (6G and 6H; points are partial residual deviances and the dotted lines represent $2 \times \text{s.e.}$). The form of the transformations is obtained by plotting the new transformed values of each variable against the original, observed values.

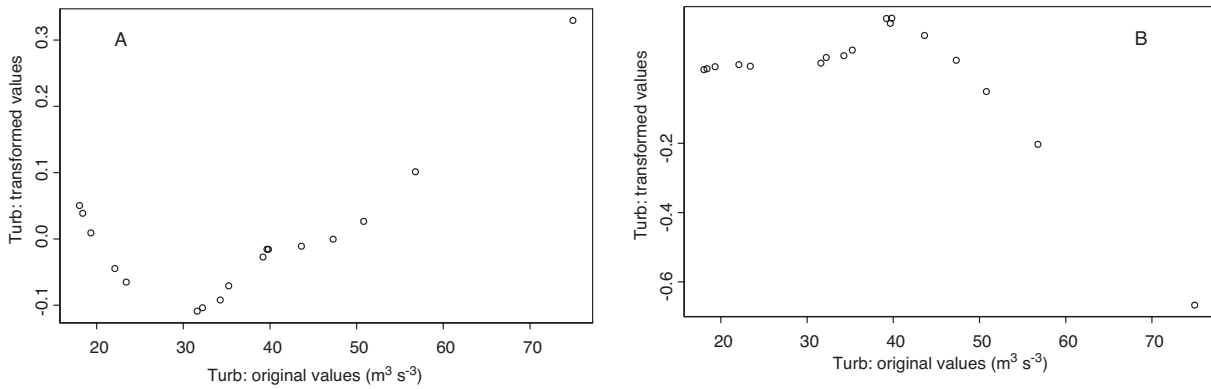


FIG. 7. – Transformations of the turbulence index through (A) ACE and (B) AVAS. The form of the transformations is obtained by plotting the new transformed values of each variable against the original, observed values.

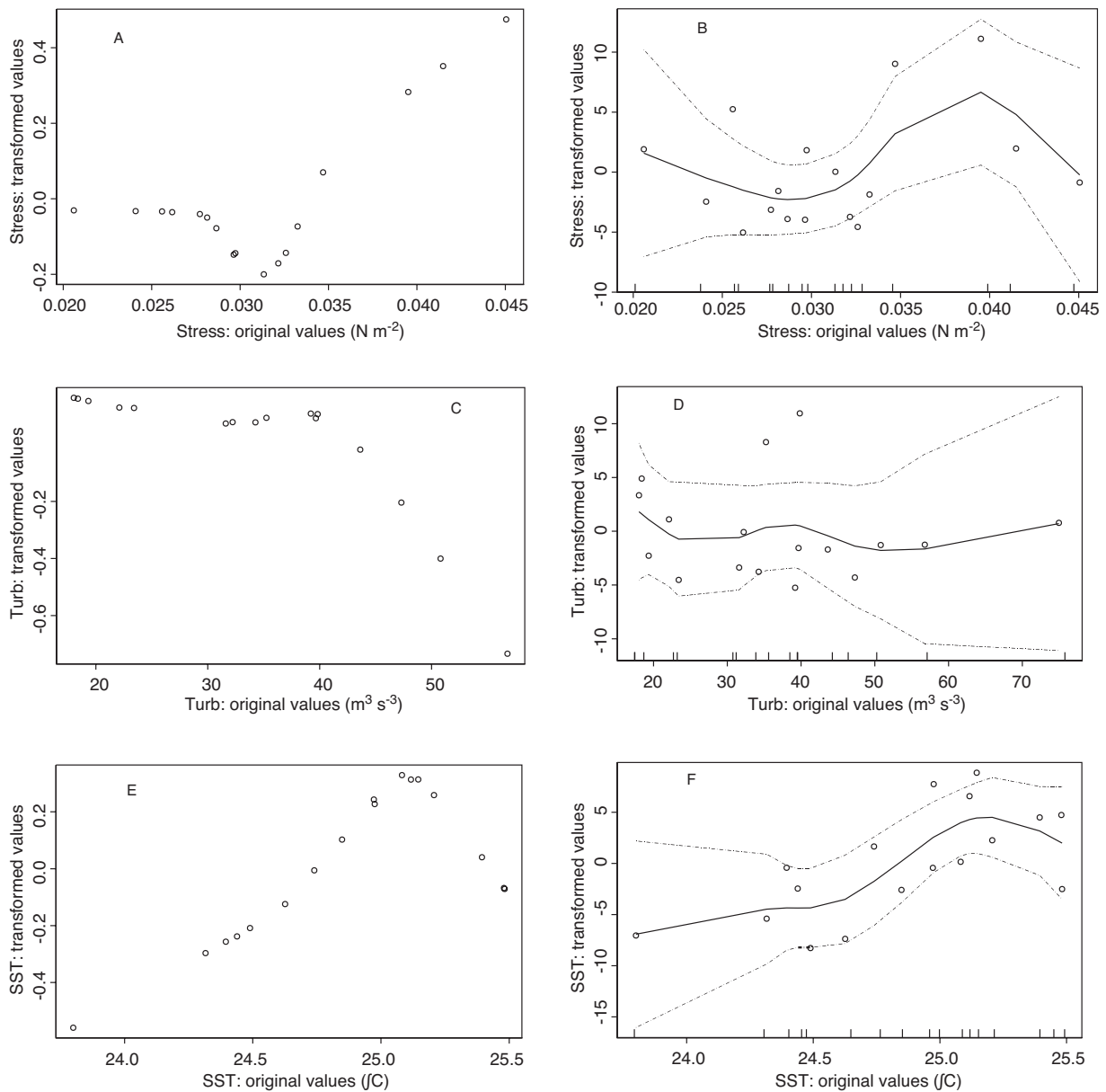


FIG. 8. – ACE transformations for (A) wind stress, (C) turbulence index, without the point for 1990, and (E) SST in combination with SSB. GAM transformations for the same variables (8B, 8D and 8F; points are the partial residual deviances and the dotted line $2 \times \text{s.e.}$). The form of the transformations is obtained by plotting the new transformed values of each variable against the original, observed values.

the point for 1990; the transformations with and without the 1990 point were similar.

For SSB and wind stress, both ACE and AVAS transformations (figure not presented) fail to show the peak that is clearly visible only in the GAM transformation (Fig. 8B).

The transformations when SSB and SST are combined as predictive variables are similar for the three methods (ACE, AVAS and GAM); their dome-shaped regions are between 24.75 and 25.5°C (transformations for ACE and GAM can be seen in Figs. 8E and 8F).

For ACE and AVAS, the quality of the fits can be measured also by the R^2 of the linear regressions between the transformed value of the response and the transformed values of the predictive variables.

The R^2 and p -values for the F -test on the regressions of the response transformations as a function of the predictor variable transformations varied from 0.84 (ACE; SSB and turbulence index) to 0.94 (ACE; SSB and Ekman) and from 0.61 (AVAS; SSB and Stress) to 0.86 (AVAS; SSB and Ekman), and the corresponding p -values from 0.0003 to 0.000002 (ACE) and from 0.001 to 0.000001 (AVAS).

When SST was included in the models together with the wind variables (Ekman, Stress or turbulence index), the R^2 for ACE and AVAS increased and the residual deviances of the GAMs decreased, indicating a better fit. When SSB, Ekman and SST were considered as predictor variables, the R^2 varied from 0.91 (ACE) to 0.93 (AVAS). The residual deviance decreased from 323 to 184 when both Ekman transport and SSB were included in the models, giving an F of 6.308 and a p -value of 0.051. The inclusion of SST brings the residual to 22, with an F of 7.301 and a p -value of 0.04. Therefore, the inclusion of each of the new predictors results in significantly better fits at an error level of 5%.

However, as shown in Figure 9, the transformations resulting from ACE (Figs. 9A and 9C) and GAM (Figs. 9B and 9D), with SST as a third regressor combined with SSB and Ekman transport, either do not show peaks or seem to be more diffuse (the same is seen with the other variables and the AVAS applications). Figure 9 only shows the transformations for Ekman transport and SST, but it is important to note that the models were applied to the three predictors (SSB, Ekman and SST) as a whole.

Although the decrease of the residual deviance in GAM applications and the increase in R^2 in most of ACE and AVAS applications indicates statistical sig-

nificance, the inclusion of SST as a third predictor variable (Figs. 9A and 9B) led to the loss of the dome-shaped regions apparent in the curves of the transformations of Ekman transport (when taken as a second predictor combined with SSB? Figs. 6E, 6F and 6H). The ACE methodology, when applied to SSB, Ekman transport and SST combined, was an exception as far as R^2 was concerned, with a decrease from 0.94 to 0.91. Such a reduction in R^2 should not occur and is probably attributable to some anomaly or instability of the ACE procedure itself. This suggests that, because of the small data set, the increase in the equivalent number of parameters determined by the inclusion of the new variable could be contributing to the distortions in the transformations.

DISCUSSION

The concept of an optimal environmental window

Cury and Roy (1989), Bakun and Nelson (1991), Roy *et al.* (1992) and Cury *et al.* (1995), comparing different stocks of anchovy and sardine in eastern wind-induced upwelling systems (Morocco, Senegal, Peru, California), found consistent evidence of the existence of an optimal environmental window related to wind intensity between 5.0 and 6.0 m s⁻¹. Dome-shaped curves would separate regions of light and strong winds, which are both unfavourable in terms of recruitment success. So far there has been no attempt to verify similar trends for stocks in western upwelling systems.

Bakun and Parrish (1990) described the oceanographic features of the region between Cabo São Tomé (22°S) and Cabo Santa Marta (29°S), based on climatological data. They demonstrated minimum wind stress and turbulence inside the Bight throughout the year. In December and January, the whole Bight was contained within a 250 m³ s⁻³ turbulence index line, corresponding to average wind speeds of <6.3 m s⁻¹. Such elements, including a stable environment characterised by a minimum turbulence, but previously enriched by the upwelling process, would favour larval survival. According to these authors, despite the very different biological context (different genera) and environmental context (tropical climate and western boundary system), there would be a high degree of similarity in the adaptive strategies of reproduction for the Brazilian sardine

and sardine off California, Africa, Chile and Peru. Nevertheless, the last four systems are notable for their marked upwelling, the offshore component of Ekman transport being $>1.5 \text{ t s}^{-1} \text{ m}^{-1}$ in the California current and $2 \text{ t s}^{-1} \text{ m}^{-1}$ in the Canary and Peru currents. Off Cabo São Tomé and Cabo Frio, the comparative value would be slightly $>0.5 \text{ t s}^{-1} \text{ m}^{-1}$ from August to January (Bakun and Parrish, 1990).

The role of SACW in the southeastern Brazilian Bight

Matsuura (1996), in his analysis of the recruitment failure of Brazilian sardine in the 1974/75 spawning season, pointed to the lack of intrusion of SACW as a main cause of the high larval mortality. Larval survival would be related to nutrient enrichment and the concentration of suitable prey subsurface, resulting from vertical stability of the water column. The existence of an optimal environmental window can therefore be linked to the intensity of the wind. Light wind would reduce the likelihood of nutrient enrichment through wind-induced upwelling or mixing, thus leading to inadequate production of larval food. On the other hand, strong-wind-driven turbulent mixing could disaggregate patches of larval food and cause excessive offshore transport, leading to loss of larvae from a favourable coastal habitat (Bakun, 1996).

A causal relationship between the SACW and wind intensity during January and February (when Brazilian sardine spawning activity is at its highest) was deduced from the results of five cruises carried out between December 1976 and January 1980. The results (Figs. 3 and 4, Tables 1 and 2) suggest that wind speeds $>3.5 \text{ m s}^{-1}$ should suffice to guarantee the SACW intrusion. The intensity of the wind in the Bight in December and January (mainly northeasterly) was quite low, some $2.5\text{--}4.5 \text{ m s}^{-1}$. Wind stress varied from 0.020 to 0.045 N m^{-2} . Similar values have been documented by Taschetto and Wainer (1999) and Sunyé (1999) on the basis of climatological data collected from 1945 to 1989.

Fitting nonparametric models

The nonparametric models applied in this paper are similar to those used by Cury and Roy (1989), Roy *et al.* (1992) and Cury *et al.* (1995). The fitting techniques are based on smoothers, but they use different procedures. In each case we aimed to achieve equilibrium when including potentially important

predictor variables along with recruitment, and at the same time we tried to minimise the number of degrees of freedom necessary for the fit.

Additive models with response transformation when applied to variables separately show the best results for spawning stock biomass (explaining 62 and 88% of recruitment variability with AVAS and ACE respectively) and Ekman transport (21 and 69% with AVAS and ACE respectively). Also, the lowest residual deviances were obtained with the GAM for Stress, Biomass and Ekman fits (Table 5).

Similar to the case for a multiple linear regression, considering the set of possible intervening variables in the recruitment process would lead to a decrease in the possible bias of estimation caused by confounding variables. When spawning stock biomass is analysed against each of the environmental predictors, the fraction of recruitment variability that is explained increases. When the models are fitted to biomass and Ekman transport, R^2 reaches 94% (ACE) and 83% (AVAS). The recruitment transformations are either approximately logarithmic or linear. For biomass, the transformations are also logarithmic. The Ekman transport transformations are almost dome-shaped, with lower and upper limits of 520 and $700 \text{ kg s}^{-1} \text{ m}^{-1}$ (Figs. 6E and 6F).

An optimal environmental window in the southeastern Brazilian Bight

If there is indeed an optimal interval for wind effects to influence recruitment, and taking the GAM transformations as a reference, limit values for wind stress would be 0.035 and 0.045 N m^{-2} and for the turbulence index 30 and $45 \text{ m}^3 \text{ s}^{-3}$ (Figs. 8B and 8D). These values, like those for Ekman transport, refer to wind speeds of $3.0\text{--}4.5 \text{ m s}^{-1}$, which are lower than those documented by Cury and Roy (1989) and Roy *et al.* (1992) for eastern boundary systems, except off Morocco, for which the optimal interval these authors gave was $4.0\text{--}5.0 \text{ m s}^{-1}$.

SST transformations are also almost dome-shaped, optimising around 24.75 and 25.5°C (Figs. 8E and 8F). These values are slightly higher than the average temperature (24.3°C) reported by Matsuura (1998) for positive stations for sardine eggs during cruises carried out from 1976 to 1993. Nevertheless, the range of temperatures of positive (sardine egg) stations given by Matsuura (1998) was $21.3\text{--}27.3^\circ\text{C}$. Matsuura also felt that his average SST was probably influenced by temperature values at stations in areas where the thermocline was shallow, thus low-

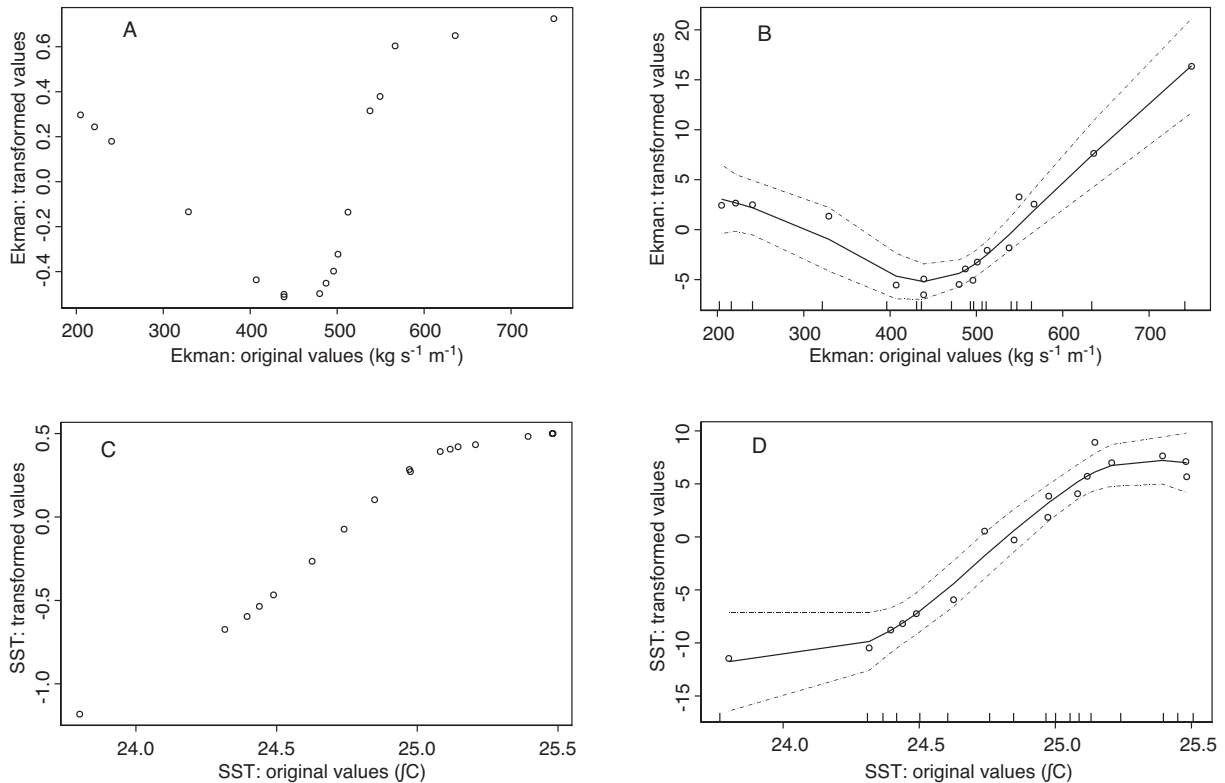


FIG. 9. – Transformations resulting from (A) ACE and (B) GAM for Ekman transport (when considered as a predictor variable together with SSB and SST), and (9C and 9D) the same results for SST. The transformations obtained with AVAS were practically identical and are not presented. The form of the transformations is obtained by plotting the new transformed values of each variable against the original, observed values.

ering the average. His median temperature distribution was around 25°C. It should also be borne in mind that temperatures from the Da Silva database refer to the surface layer, and re perhaps slightly different from those taken 10 m deep.

Possible anomalies in the application of the models

The attempt to include SST as a new predictor in fitting, despite an increase in R^2 , clearly caused the loss of the dome shape in the relationship in almost all transformations (Figs. 9A, 9B, 9C and 9D). One possible explanation for this is that the scarceness of observations directly affects the quality of the resulting curves. This explanation would be particularly relevant when a greater number of predictor variables are included, thus triggering an increase in the equivalent number of parameters required for the fit. When considering three predictors, the number of residual degrees of freedom decreases to 4, indicating that it was necessary to use 13 d.f. for the fit, 4 parametric (one for the intercept and one for each predictor) and 9 nonparametric (3 for each variable). Even though a fit is still possible with 13 observa-

tions (because we have 17 points), we are clearly approaching the limit of applicability of the models to this set of data.

The results suggest that the models can behave in an unusual fashion when the required number of degrees of freedom is high compared with the total number of observations. This does not imply that SST must be rejected as a third regressor and as a possible factor influencing recruitment, but it does demonstrate that it can distort the output from additive models when it is included, given the small number of available observations.

As the water derived from the SACW intrusion does not reach the sea surface except where upwelling is relatively strong, inclusion of SST in the models reflects biological effects different from those related to wind intensity. SST optimal intervals would be related to the spawning process itself (occurrence of spawning, hatching and larval survival).

The critical minimum spawning stock biomass

Quantitative modelling of Brazilian sardine recruitment has shown in all cases the importance of

a sufficiency of spawning stock biomass. Despite the various transformation forms and the method applied (ACE, AVAS or GAM), we found curves close to logarithmic, 250,000 t being the limit between the linear portion and the interval where recruitment is fairly constant in relation to the size of the spawning stock. The form of the curve is similar to those proposed by Cergole (1995) and Vasconcellos (2000). Cergole (1995) and Cergole *et al.* (2002) suggest that a spawning stock biomass of some 180,000 t would be a critical minimum size; below that, its maintenance would be strictly dependent on recruitment success. IBAMA (2000) suggest that the minimum spawning stock biomass to guarantee sustainability would be of the order of 120,000 t.

CONCLUSIONS

We believe that we have shown that the wind and upwelling-based system in the southeastern Brazilian Bight, despite generally light winds in summer, reveals an optimal environmental window for wind intensities between 3.0 and 4.5 m s⁻¹. The evidence leads us to believe that even the limited turbulence arising from winds stronger than 4.5 m s⁻¹ can disrupt the plankton distribution pattern that is crucial for survival of sardine larvae in the Bight.

Although wind intensity and SST are relatively important in explaining recruitment variability, the effects derived from them are less important than the size of the spawning stock biomass. In terms of optimising recruitment success, evaluation of the biomass transformations revealed a critical minimum value for spawning stock biomass of 200,000-250,000 t. Such a conclusion is important for stock management, pointing to the necessity to adopt strategies of conservation based on the size of the spawning stock biomass, including implementing effective control of fishing effort or establishing quotas. Currently, stock management of Brazilian sardine is limited to closed seasons (30-45 days during the peak spawning season), a minimum size (17 cm), and an attempt to control fishing effort through granting special permissions (Sunyé, 1999; IBAMA, 2000).

Nonparametric models seem to be efficient identifiers of possible forms of the relationships between predictor variables and recruitment response. However, they suffer from the small size of the available data set and behave strangely in some applications. New observations and longer time-series would

allow for more consistent tests, with the inclusion of all potential regressors.

ACKNOWLEDGEMENTS

We thank Dr. Yasunobu Matsuura, coordinator of the FINEP Project developed by the Instituto Oceanográfico da USP (IOUSP) with funds from Financiadora de Estudos e Projetos S/A (FINEP), for providing the water column temperature data, and Marizilda Magro for her tabulation of the temperature data. Special thanks are also due to Drs. Maria Cristina Cergole and Carmen Rossi-Wongtschowski of the Institute of Oceanography, University of São Paulo, and two anonymous reviewers for valuable comments on earlier versions of the manuscript.

REFERENCES

- Bakun, A. – 1996. *Patterns in the Ocean. Ocean Processes and Marine Population Dynamics*. University of California Sea Grant, San Diego, California, USA, in cooperation with Centro de Investigaciones Biológicas de Noroeste, La Paz, Baja California Sur, Mexico, 323 pp.
- Bakun, A. and C.S. Nelson. – 1991. The seasonal cycle of wind-stress curl in subtropical eastern boundary current regions. *J. phys. Oceanogr.*, 21: 1815-1834.
- Bakun, A. and R.H. Parrish. – 1990. Comparative studies of coastal pelagic fish reproductive habitats: the Brazilian sardine (*Sardinella aurita*). *J. Cons. int. Explor. Mer*, 46: 269-283.
- Beverton, R.J.H. and S.J. Holt. – 1957. On the dynamics of exploited fish populations. *Fishery Invest., Ser. II*, London, 19, 533 pp.
- Bloomer, S.F., K.L. Cochrane and J.G. Field. – 1994. Towards predicting recruitment success of anchovy *Engraulis capensis* Gilchrist in the southern Benguela system using environmental variables: a rule-based model. *S. Afr. J. mar. Sci.*, 14: 107-119.
- Breiman, L. and J.H. Friedman. – 1985. Estimating optimal transformations for multiple regression and correlation (with discussion). *J. Am. statist. Assoc.*, 80: 580-619.
- Cergole, M.C. – 1993. *Avaliação do estoque da sardinha verdadeira, Sardinella brasiliensis da costa sudeste do Brasil, período 1977 a 1990*. PhD thesis. Universidade de São Paulo, Instituto Oceanográfico.
- Cergole, M.C. – 1995. Stock assessment of the Brazilian sardine, *Sardinella brasiliensis*, of the south-eastern coast of Brazil. *Sci. Mar.*, 59(3-4): 597-610.
- Cergole, M.C., S.A. Saccardo and C.L.D.B. Rossi-Wongtschowski. – 2002. Fluctuations in the spawning stock biomass and recruitment of the Brazilian sardine (*Sardinella brasiliensis*). 1977-1997. *Rev. bras. oceanogr.*, 50(1) (in press).
- Cury, P. and C. Roy. – 1989. Optimal environmental window and pelagic fish recruitment success in upwelling areas. *Can. J. Fish. aquat. Sci.*, 46(4): 670-680.
- Cury, P., C. Roy, R. Mendelsohn, A. Bakun, D.M. Husby and R.H. Parrish. – 1995. Moderate is better. Nonlinear climatic effect on California anchovy. In: R. J. Beamish (ed.). *Climate Change and Northern Fish Populations*, pp. 417-424. *Can. Spec. Publ. Fish. aquat. Sci.*, 121, 739 pp.
- Da Silva, A., A.C. Young and S. Levitus. – 1994. *Atlas of Surface Marine Data 1994. 1. Algorithms and Procedures*. NOAA Atlas NESDIS 6, U.S. Department of Commerce, Washington, D.C.
- Gulland, J.A. – 1965. Estimation of mortality rates. Annex to Arctic fisheries working group report. *ICES C.M. Doc.* 3 (mimeo).

- Hastie, T.J. and R.J. Tibshirani. – 1990. *Generalized Additive Models*. Chapman & Hall, London.
- IBAMA. – 2000. Relatório da reunião técnica sobre o estado da arte e ordenamento da pesca de sardinha-verdadeira (*Sardinella brasiliensis*) nas regiões sudeste e sul. Itajaí, IBAMA/CEPSUL, 27 pp.
- Matsuura, Y. – 1996. A probable cause of recruitment failure of the Brazilian sardine *Sardinella aurita* population during the 1974/1975 spawning season. *S. Afr. J. mar. Sci.*, 17: 29-35.
- Matsuura, Y. – 1998. Brazilian sardine (*Sardinella brasiliensis*) spawning in the southeast Brazilian Bight over the period 1976-1993. *Rev. bras. oceanogr.*, 46(1): 33-43.
- Matsuura, Y. – 1999. Large scale fluctuations of small pelagic fish populations and climate change. A review. *Bull. Tohoku nat. Fish. Res. Inst.*, 62, 11 pp.
- Pauly, D. – 1980. On the interrelationships between natural mortality, growth parameters, and mean environmental temperature in 175 stocks. *J. Cons. int. Explor. Mer*, 39(2): 175-192.
- Roy, C., P. Cury and S. Kifani. – 1992. Pelagic fish recruitment success and reproductive strategy in upwelling areas: environmental compromises. In: A.I.L. Payne, K.H. Brink, K.H. Mann and R. Hilborn (eds.). *Benguela Trophic Functioning*, pp. 135-146. *S. Afr. J. mar. Sci.*, 12.
- S-PLUS 4 - 1997. *Guide to Statistics*. Data Analysis Products Division, MathSoft, Seattle.
- Sunyé, P.S. – 1999. *Effet de la variabilité climatique régionale sur la pêche de la sardinelle le long de la côte sud-est du Brésil (1964-1993)*. PhD thesis. Université de Bretagne Occidentale, Institut Universitaire Européen de la Mer, 130 pp.
- Taschetto, A.S. and I. Wainer. – 1999. *Estudo climatológico da ressurgência na região sudoeste do Atlântico sul*. 23 pp. (mimeo).
- Tibshirani, L. – 1988. Estimating optimal transformations for regression via additivity and variance stabilisation. *J. Am. statist. Assoc.*, 83: 394-405.
- Vasconcellos, M. – 2000. *Ecosystem impacts of fishing forage fishes. An analysis of harvest strategies for the Brazilian sardine*. Thesis submitted in partial requirements for the degree of Doctor of Philosophy, Faculty of Graduated Studies, University of British Columbia, Vancouver, Canada.
- Yoneda, N.T. – 1987. *Criação em laboratório de larvas da sardinha-verdadeira *Sardinella brasiliensis* e estudo dos incrementos diários nos otólitos*. MSc dissertation, Universidade de São Paulo, Instituto Oceanográfico.
- Scient. ed.: A.I.L. Payne